

# Theory of Weak-Shocks Interactions with Transonic Mixing Layers

César Huete, Antonio L. Sánchez, Forman A. Williams  
University of California San Diego  
La Jolla, California 92093-0411, USA

Javier Urzay  
Stanford University  
Stanford, CA 94305-3024, USA

## 1 Introduction

Mixing layers and shock waves are two different phenomena that coexist in hypersonic and supersonic propulsion devices. For instance, in supersonic-combustor ramjets, shock waves are typically generated ahead of the combustion zone, where the supersonic incoming flow enters a converging nozzle and interacts with wedged walls and fuel injectors. Along its path through the combustor, the flow is subject to complex shock trains and expansion waves [1]. In one configuration, the shock waves may interact with the mixing layer generated downstream from the fuel injector, which separates the supersonic incoming hot-air stream and the subsonic fuel flow. Since the residence time of the reactants in the combustor is short in supersonic regimes, ignition typically cannot be achieved by relying on diffusion and heat conduction alone [2]. Shock waves may help, however, to heat the mixture and speed the mixing process [3–6], the former arising from the inherent temperature rise across the shock wave, and the latter associated with the interaction of the shock with the non-uniform flow.

Analytical solutions to related simplified problems can be helpful in studying such supersonic-combustion processes, not only for increasing understanding but also for suggesting scaling concepts that may prove useful. The present work, which is of that type, pertains to laminar mixing layers subjected to impingement by shocks that are sufficiently weak to be treated as perturbations, thereby facilitating pure, analytical approaches that would not be feasible if the nonlinearities associated with finite shock intensities or with turbulent flow were present. With that in mind, the theory of interaction of weak shocks with transonic mixing layers is addressed here. As a first step, an inert mixing layer is considered, the influence of the shock on the combustion and heat release being deferred to later investigations. A crucial asset for the present investigation is the earlier work of Lighthill [7, 8] and Riley [9] on weak-shock impingement on boundary layers and mixing regions, respectively. This type of problem, involving linear (weak-shock) perturbations of a laminar viscous region at large values of the Reynolds number,  $Re$ , can be treated rigorously through matched asymptotic expansions for  $Re$  approaching infinity, resulting in a triple-deck theory [10]. The mixing-layer problem to be addressed here turns out to be a particularly simple version of multi-scale problems of this type, for example because it is unnecessary to deal with the bottom (low-speed, viscous, incompressible) deck.

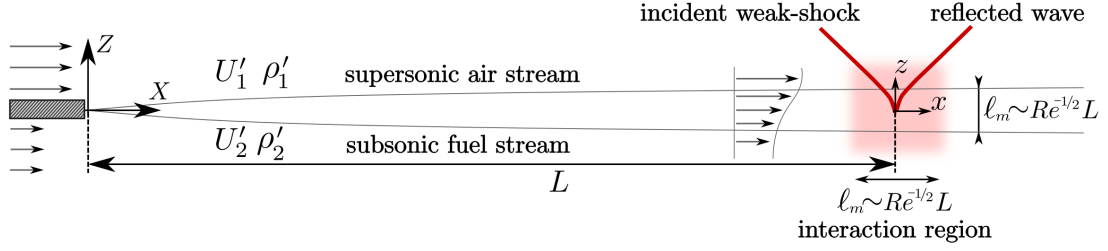


Figure 1: Sketch of the problem.

## 2 The transonic mixing layer

We consider the interaction of a steady transonic mixing layer -separating a supersonic air stream from a subsonic fuel stream- with a small, external, steady, pressure perturbation approaching from the supersonic side. The mixing layer develops downstream from a separating splitter plate, with the perturbation reaching the mixing layer at a downstream distance  $X = L$ , as indicated in figure 1. The distribution of flow properties across the laminar mixing layer depends on the type of air-fuel mixture, with two different relevant cases considered below. A first set of integrations neglects variations of the mean molecular weight and assumes a unity Lewis number when describing the fuel diffusion velocity, with thermal diffusion neglected. This case, termed the simplified case below, is representative of fuels that have properties close to those of air, such as ethylene. Investigation of hydrogen, a more promising candidate for high-speed combustion because of its favorable chemical properties (high mass-based energy density and high reactivity), requires a separate analysis including consideration of its specific physical properties, i.e., low molecular weight, high diffusivity, and non-negligible thermal diffusion.

The relevant Reynolds number of the flow  $Re = \rho'_1 U'_1 L / \mu'_1$ , based on the velocity  $U'_1$ , density  $\rho'_1$ , and shear viscosity  $\mu'_1$  of the supersonic stream is assumed to be moderately large and comparable in magnitude to the corresponding value  $\rho'_2 U'_2 L / \mu'_2$  based on the subsonic-stream properties. This results in a slender mixing layer, whose characteristic thickness increases according to  $[(\mu'_1 / \rho'_1) X / U'_1]^{1/2}$ , reaching a value  $\ell_m$  of order  $Re^{-1/2} L \ll L$  at  $X = L$ .

In the absence of external perturbations, the transonic mixing layer that develops downstream from the splitter plate possesses a selfsimilar solution in terms of the rescaled transverse coordinate  $\eta = Z / [(\mu'_1 / \rho'_1) X / U'_1]^{1/2}$ . In the description, the longitudinal and transverse velocity components are scaled with their characteristic values  $U'_1$  and  $[(\mu'_1 / \rho'_1) U'_1 / X]^{1/2}$  to define the nondimensional functions  $U(\eta)$  and  $V(\eta)$ , while the temperature and density are scaled with their air-side values  $T'_1$  and  $\rho'_1$ , respectively, to define  $T(\eta)$  and  $R(\eta)$ . Since the ratio  $\gamma$  of specific heats is essentially constant in these ideal-gas mixtures, the sound speed is inversely proportional to the square root of the density because the pressure does not vary appreciably across the mixing layer. As a result, the distribution of Mach number  $M(\eta)$  can be evaluated from the nondimensional velocity and density profiles according to  $M(\eta) = M_1 U(\eta) R(\eta)^{1/2}$ , where  $M_1 > 1$  is the Mach number of the air stream, yielding the relation  $M_2 = M_1 U_2 R_2^{1/2} < 1$  for the fuel-stream Mach number. Since the interactions investigated below depend fundamentally on the Mach-number distribution, it seems appropriate to use the condition of achievement of 99% of the free-stream Mach number as the defining criterion for the location of the upper and lower edges of the mixing layer  $\eta_1$  and  $\eta_2$ . Correspondingly, the analysis yields the value  $\ell_m = (\eta_1 - \eta_2) [(\mu'_1 / \rho'_1) L / U'_1]^{1/2}$  for the mixing-layer thickness at  $X = L$ , to be used below as a scale for the interaction region.

As nitrogen and oxygen are very similar, they will be treated below as a single species, thereby reducing

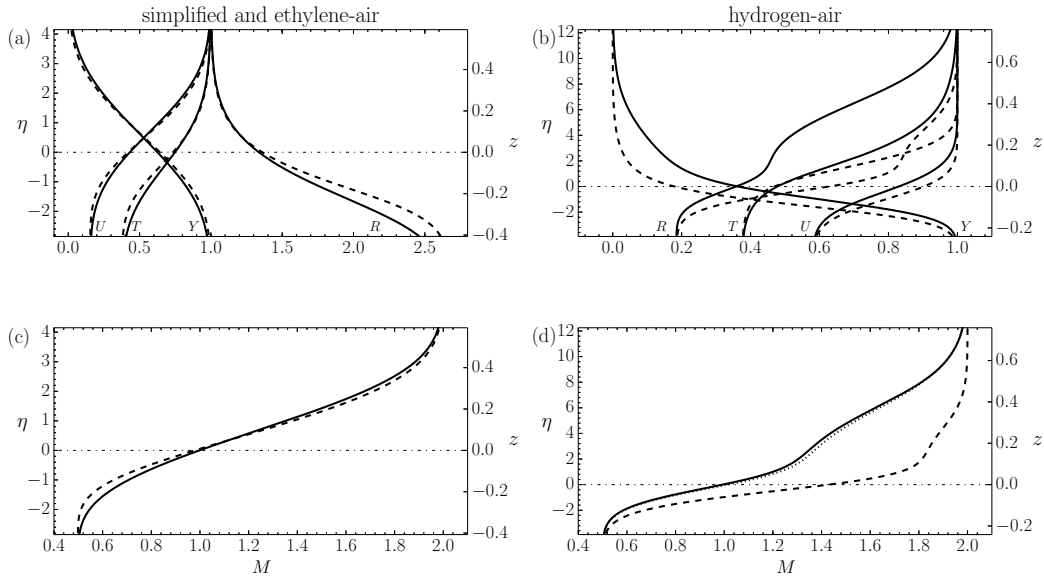


Figure 2: Profiles of  $U$ ,  $T$ ,  $R$ ,  $Y$ , and  $M$  for simplified and ethylene-air mixing layers (left-hand-side plots) and for a hydrogen-air mixing layer (right-hand-side plots) with  $T_2 = 0.375$ ,  $M_1 = 2$  and  $M_2 = 0.5$ . In panels (a) and (c), the solid and dashed curves represent the simplified and ethylene-air cases, respectively; in panels (b) and (d), the dashed and dotted curves represent results obtained by removing the Soret and Dufour effects, respectively.

the mixing process to that of a binary mixture, with the local composition characterized in terms of the fuel mass fraction  $Y$ . The corresponding fuel diffusion flux accounts for both species gradient diffusion and thermal diffusion, the latter having a significant effect for hydrogen [12].

Sample profiles of  $U$ ,  $T$ ,  $R$ , and  $Y$  obtained for the case  $T_2 = 0.375$  with  $M_1 = 2$  and  $M_2 = 0.5$  are shown in figure 2, which also displays the corresponding distributions of Mach number. The results for the simplified case, shown as solid curves in the left-hand-side plots, are compared with the computations employing the specific properties of ethylene (i.e.,  $Le = 1.2$ ,  $W_2 = 0.97$ , and  $\mu'_2 = 0.6\mu'_1$ ). In view of the small differences observed, especially in connection with the resulting Mach-number distributions, it can be concluded that the simplified case is a realistic representation of fuel-air mixing layers involving light hydrocarbons fuels, such as ethylene. The results shown in figures 2 (a) and 2 (c) appear to be quite symmetric, while those for hydrogen-air systems are more irregular, exhibiting, for example, three inflection points in the profiles of density and Mach number. These differences are due to the specific properties of hydrogen, notably its low molecular weight and high diffusivity.

### 3 Interaction with a weak shock

The interactions of the external pressure perturbation with the mixing layer will be studied in a reference frame whose origin is placed at the intersection of the incident wave with the sonic line, located at  $(X, Z) = (L, Z^*)$ . Using  $\ell_m$  as characteristic length results in the local coordinates  $x = (X - L)/\ell_m$  and  $z = (Z - Z^*)/\ell_m$ . In the interaction region, the streamwise variations of the velocity, density, temperature, and fuel mass fraction of the unperturbed base flow are small, of order  $Re^{-1/2}$ , and they can be therefore neglected in the first approximation, along with the departures of the base-flow pressure from the ambient value  $p'_o$ , of order  $Re^{-1}$ . The external pressure perturbation introduced is assumed to

be of order  $\epsilon p'_o$ , leading to relative departures from the base flow of order  $\epsilon$  given by

$$\begin{aligned} \frac{u'}{U'_1} &= U(z) + \epsilon u(x, z), & \frac{v'}{U'_1} &= Re^{-1/2}V(z) + \epsilon v(x, z), \\ \frac{\rho'}{\rho'_1} &= R(z) + \epsilon \rho(x, z), & \frac{p' - p'_o}{\gamma p'_o} &= \epsilon p(x, z), \end{aligned}$$

where the base profiles  $U(z)$ ,  $V(z)$ ,  $R(z)$  can be evaluated from the selfsimilar profiles  $U(\eta)$ ,  $V(\eta)$ ,  $R(\eta)$  with use made of  $z = \eta/(\eta_1 - \eta_2)$ . Since the local Reynolds number in the interaction region  $\rho'_1 U'_1 \ell_m / \mu'_1$  is large, of order  $Re^{1/2} \gg 1$ , the perturbations are governed by the Euler equations, which can be linearized about the base-flow solution to yield, after linear combination, a single relationship for the pressure perturbation field, namely

$$\frac{\partial^2 p}{\partial z^2} + (1 - M^2) \frac{\partial^2 p}{\partial x^2} - \frac{\partial \ln M^2}{\partial z} \frac{\partial p}{\partial z} = 0 \quad (1)$$

which depends fundamentally on the shape of the Mach-number distribution  $M(z)$ . Following Lighthill, to simplify the treatment we assume that the mixing layer extends across the finite domain  $z_2 < z < z_1$  and that the base flow is uniform outside. The problem then reduces to that of integrating (1) in  $z_2 < z < z_1$  subject to the condition that  $p$  decays as  $x \rightarrow \pm\infty$  and to the additional boundary conditions at  $z = z_1$  and  $z = z_2$  obtained from matching with the pressure field in the uniform streams.

The specific response to a weak shock can be investigated by considering an incident pressure jump defined by the Heaviside step function  $f_1 = \mathcal{H}(x + \beta_1 z + s_1 - \beta_1 z_1)$ , where  $\beta_1 = (M_1^2 - 1)^{1/2}$ . The solution of the pressure perturbation field can be obtained analytically by Fourier-transform techniques in the limits of high-frequency and small-frequency perturbations. The former, which is appropriate in describing sudden perturbations such as weak shocks, will be employed in the present analysis to study the high-frequency pressure perturbations, although the corresponding Fourier-transform algebra will be omitted in this brief presentation.

The analysis provides, in particular, the spatial distributions of the high-frequency perturbations in the supersonic and subsonic domains away from the sonic line

$$p(x, z) = \sqrt{\frac{\beta_1}{\beta} \frac{M}{M_1}} \begin{cases} \mathcal{H}(x + s), & \text{if } x < s \\ -\tilde{\gamma}\pi^{-1} - \ln(x - s)\pi^{-1}, & \text{if } x > s \end{cases} \quad (2)$$

and

$$p(x, z) = \frac{1}{\pi} \sqrt{\frac{\beta_1}{2|\beta|} \frac{M}{M_1}} \left[ \frac{\pi}{2} - \tilde{\gamma} - \ln\left(\sqrt{|s|^2 + x^2}\right) - \tan^{-1}\left(\frac{x}{|s|}\right) \right] \quad (3)$$

in which

$$\beta = (M^2 - 1)^{1/2}, \quad \text{and} \quad s = \int_0^z \beta(z') dz'. \quad (4)$$

The symbol  $\tilde{\gamma}$  refers to the Euler-Mascheroni constant. The pressure perturbation along the sonic line is found to be

$$p(x, 0) = \frac{\sqrt{\beta_1}}{\sqrt{2}M_1 [M_z(0)]^{1/6}} \left[ \frac{6^{1/3}(1/6)! \sqrt{2 + \sqrt{3}}}{(-1/3)!} \right] \left[ 1 + \frac{1 - (2 - \sqrt{3}) \operatorname{sgn}(x)}{|x|^{1/6}} \right]. \quad (5)$$

The expressions (2) and (3) for the supersonic and subsonic domains and the intermediate sonic-line pressure distribution (5) are represented in figure 3 (a-f) for the simplified and hydrogen-air mixing

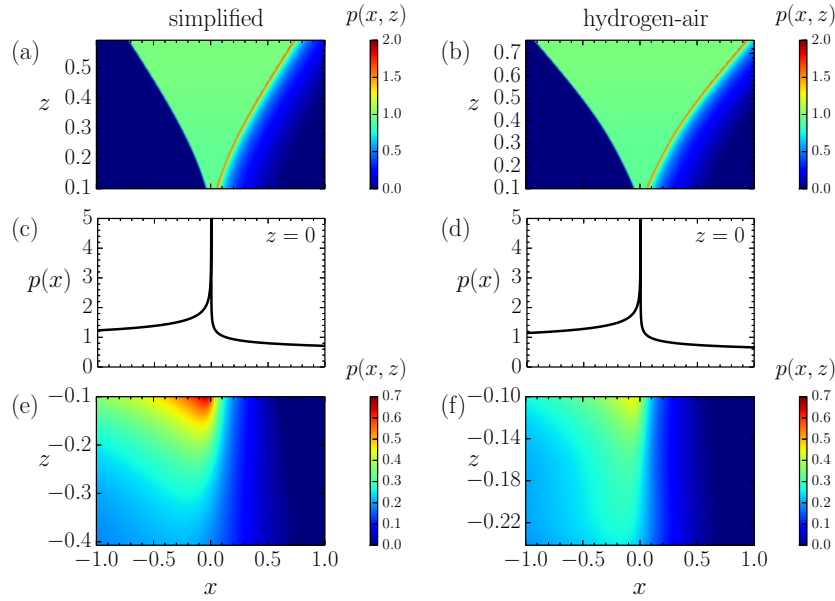


Figure 3: Pressure perturbation obtained from (a,b) equation (2) for the supersonic side, (c,d) equation (5) corresponding to the sonic line, and (e,f) equation (3) for the subsonic side, for the simplified (left-hand side) and hydrogen-air (right-hand side) Mach-number distributions of figure 2 (c,d).

layers. The trajectories of the incident and reflected waves in the supersonic stream and the distributed pressure disturbances in the subsonic stream are qualitatively similar for both mixing layers, although quantitative differences arise from the associated differences in Mach-number distribution displayed in figure 2 (c,d). Along the sonic line, however, the streamwise pressure distributions are practically indistinguishable, because the values of  $[M_z(0)]^{1/6}$  in (5) happen to be approximately equal for these two configurations. The logarithmic singularity of the reflected wave and the algebraic singularity  $|x|^{-1/6}$  at the point of incidence, both of which also are present in the original boundary-layer analysis of [7], appear to be inconsistent with the hypothesis of small disturbances. They emerge in the linear theory as a consequence of the discontinuous nature of the incident pressure wave. It is naturally expected that, in realistic configurations, the singularity would disappear as a consequence of nonlinear effects acting locally.

Although the results above are given only for the pressure perturbation, it is straightforward to compute the remaining thermodynamic variables by making use of the isentropic-flow condition. Of particular interest in this context is the associated temperature perturbation, which can potentially promote ignition when the chemical reactions have a strong temperature sensitivity. Since the deflection of the stream lines has a negligible influence on the high frequency component of the temperature perturbations, the corresponding isentropic condition reduces to  $\theta = (\gamma - 1)Tp$ , thereby giving a temperature spatial distribution qualitatively similar to that shown in figure 3 for the pressure.

Although, unlike the work of Butsworth [11], only weak shocks are addressed in this study, the results can be used to examine trends of induced effects in applications involving shock-wave ignition of fuel-air mixing-layer flows, of interest for combustion processes in supersonic engines. The interaction of the pressure wave leads to an additional indirect (although possibly important) effect associated with the local generation of vorticity, which may promote the instability of the mixing-layer flow, thereby enhancing the combustion rate by increasing the downstream mixing rate of the two streams. Alternatively, this effect could also reduce the vorticity and thereby inhibit instability and its associated turbulent

mixing. In particular, the vorticity equation can be expressed as

$$\frac{\partial \omega}{\partial x} = -\Omega \frac{\partial p}{\partial x} - \frac{U_{zz}}{U} v \quad (6)$$

where  $\Omega$  measures the collective effects of flow stretching and baroclinic torque.

For the hydrogen-air mixing layer, both  $U_z$  and  $R_z$  are positive, with the result that flow stretching and baroclinic torque cooperate to create vorticity of the same sign. The resulting function  $\Omega$  is everywhere positive. For the simplified mixing layer with constant molecular weight, however,  $R_z < 0$ , because the density is inversely proportional to the temperature and the air stream is hotter. In this case, the competition of flow stretching and baroclinic torque causes the resulting function  $\Omega$  to be predominantly negative in the subsonic domain, where the baroclinic torque is dominant, and positive in the supersonic domain, where flow stretching prevails. According to (6), vorticity can be either created or destroyed depending on the sign of the product  $-\Omega \partial p / \partial x$ , the  $U_{zz}$  term being smaller. It can be concluded from the pressure fields shown in figure 3 that at any given transverse location  $z$  there is an upstream region of adverse pressure gradient ( $\partial p / \partial x > 0$ ), including a finite pressure jump across the shock in the supersonic stream, and a downstream region of favorable pressure gradient ( $\partial p / \partial x < 0$ ).

## References

- [1] LAURENCE, S. J., KARL, S., SCHRAMM, J., MARTÍNEZ, J. & HANNEMANN, K. 2013 Transient fluid-combustion phenomena in a model scramjet. *J. Fluid Mech.* **722**, 85–120.
- [2] GUTMARK, E. J., SCHADOW, K. C., & YU, K. H. 1995 Mixing enhancement in supersonic free shear flows. *Ann. Rev. Fluid Mech.*, **27**, 375–417.
- [3] BRUMMUND, U. & NUDING, J. R. 1997 Interaction of a compressible shear layer with shock waves - an experimental study. *AIAA Paper*, **97**, 0392.
- [4] LU, P. J. & WU, K. C. 1991 On the shock enhancement of confined supersonic mixing flows. *Phys. Fluids A*, **3**, 3046–3062, 1991.
- [5] MARBLE, F. E. 1994 Gasdynamic enhancement of nonpremixed combustion. *Proc. Combust. Inst.*, **25**, 1–12, 1994.
- [6] MENON, S. 1989 Shock-wave-induced mixing enhancement in scramjet combustors. *AIAA Paper*, 89-0104.
- [7] LIGHTHILL, M. J. 1950 Reflection at a laminar boundary layer of a weak steady disturbance to a supersonic stream, neglecting viscosity and heat conduction. *Quarter. J. Mech. Appl. Math.*, **3**, 303–325.
- [8] LIGHTHILL, M. J. 1953 On boundary layers and upstream influence. II. Supersonic flows without separation. *Proc. Royal Soc. London. Series A.*, **213**, 478–507.
- [9] RILEY, N. 1960 Interaction of a shock wave with a mixing region. *J. Fluid Mech.* **7**, 321–339.
- [10] NAYFEH, A. H. 1991 Triple-deck structure. *Computers Fluids*, **20**, 269–292.
- [11] BUTTSWORTH, D. R. 1996 Interaction of oblique shock waves and planar mixing regions. *J. Fluid Mech.* **306**, 43–57.
- [12] SÁNCHEZ, A. L. & WILLIAMS, F. A. 2014 Recent advances in understanding of flammability characteristics of hydrogen. *Prog. Energy Combust. Sci.*, **41**, 1–55.